

## Self-Guiding of Ultrashort, Relativistically Intense Laser Pulses through Underdense Plasmas in the Blowout Regime

J. E. Ralph, K. A. Marsh, A. E. Pak, W. Lu, C. E. Clayton, F. Fang, W. B. Mori, and C. Joshi

*Department of Electrical Engineering, UCLA, Los Angeles, California 90095, USA*

(Received 11 September 2008; published 30 April 2009)

The self-guiding of relativistically intense but ultrashort laser pulses has been experimentally investigated as a function of laser power, plasma density, and plasma length in the blowout regime. The extent of self-guiding, observed by imaging the plasma exit, is shown to be limited by nonlinear pump depletion with observed self-guiding of over tens of Rayleigh lengths. Spectrally resolved images of the plasma exit show evidence consistent with self-guiding in the plasma wake. Minimal losses of the self-guided pulse resulted when the initial spot size was matched to the blowout radius.

DOI: 10.1103/PhysRevLett.102.175003

PACS numbers: 52.38.Kd, 41.75.Jv, 52.35.Mw

It is recognized that excitation of strong wakes traveling near light speed in centimeter-scale plasmas is crucial for realizing a “benchtop,” GeV-class laser-wakefield accelerator (LWFA) [1]. Such wakes are formed when a relativistically intense and ultrashort laser pulse propagates through an underdense plasma [2]. Extending the interaction length of such pulses, without the need to propagate them through a *preformed* plasma density channel [3–5], would greatly simplify a practical LWFA device. There have been limited systematic prior experimental studies of the self-guided blowout regime, although many current laser-wakefield experiments rely on this mechanism to extend the acceleration length [6]. In recent studies, self-guiding was observed using a 2 mm gas jet [7–9], but no limiting mechanism was demonstrated. Extending this self-guided length with higher laser powers and lower plasma densities holds the promise of obtaining multi-GeV energy electron beams from a LWFA [10].

In this Letter we show that it is possible to self-guide such a laser pulse and continue to excite a wake over tens of Rayleigh lengths  $Z_R$  in the so-called blowout regime [2,11,12]. Furthermore, we have determined a scaling of the length over which such a pulse can be guided as a function of the ambient electron plasma density  $n_e$  and deduce that this length is consistent with the nonlinear pump depletion length  $L_{pd}$ . This observed limitation can also explain the limited experimental lengths reported in other short-pulse self-guiding studies [5,13]. Finally, optimal self-guiding was found when  $n_e$ , laser power  $P$ , and the original laser spot size  $w_o$  are matched according to recent theory [2].

Matched guiding of a laser pulse occurs when diffraction is balanced by focusing. In a plasma, this occurs when there is a radial variation of the electron density that provides the normalized on-axis depression  $\delta n/n_e \approx 4/(k_p^2 w_0^2)$ , which in turn produces a refractive index channel that guides the pulse [14]. Here  $k_p$  is the plasma wave number. In the blowout regime, the laser pulse’s initial

ponderomotive force causes  $\delta n/n_e \approx 1$  within the pulse [15] which modifies the matching condition.

When a relativistically intense  $a_o \geq 1$  but ultrashort  $c\tau \approx \lambda_p$  laser pulse with power  $P > P_c$  enters an underdense,  $\omega_p < \omega_o$ , plasma, the plasma electrons at the head of the pulse are completely blown out radially during the rise time of the pulse leaving an ion channel in the first plasma period. Here  $a_o = eA/mc^2$  is the normalized vector potential of the laser,  $\omega_o$  and  $\omega_p$  are the laser and plasma frequencies, respectively,  $\tau$  is the full width half maximum (FWHM) of the duration of the laser pulse,  $\lambda_p = 2\pi c/\omega_p$  and  $P_c \approx 17(\omega_o/\omega_p)^2$  GW which is the critical power for relativistic self-focusing [14]. The plasma ions exert an attractive force on these electrons which then rush back toward the laser axis setting up the wakefield. Most of the laser pulse thus resides inside the electron density depression and can therefore be guided. However, due to the inertia of the electrons, the density or refractive index channel is expected to form on a longitudinal scale length of  $c/\omega_p$ . Therefore the very front of the laser pulse continuously erodes away due to diffraction with the degree of guiding of the remaining pulse varying along the laser pulse [16]. An estimate of the erosion rate is often quoted as  $c/\omega_p$  per  $Z_R$  which would limit the distance over which such an ultrashort pulse can be self-guided to a few  $Z_R$  [14]. However, nonlinear theory [11] and more recent 3D phenomenological theory [17] of LWFA show that in spite of diffractive erosion, self-guiding and wake excitation is indeed possible over tens of  $Z_R$  in the blowout regime.

To achieve such self-guiding in the blowout regime over a distance for significant acceleration,  $w_0$  must be matched to the blowout radius  $R_b$  of the electrons so that  $k_p w_o \approx k_p R_b \approx 2\sqrt{a_o}$ . For a matched spot  $w_m \approx R_b$ , this can be expressed as  $k_p w_m = 2\sqrt{2}(P/P_c)^{1/6}$ . It has been shown that for  $P/P_c > 1$  and  $w_o > w_m$ , the spot size will converge to (and remain at)  $w_m$  [2,7] where diffraction at the head of the laser pulse is minimized. As  $w_o$  is reduced from the

matched spot size, diffraction loss tends to increase [2]. As a matched ultrashort laser pulse with  $a_0 \geq 2$  propagates through the plasma, the front of the laser pulse locally pump depletes as the wake is excited causing the photons to shift to longer wavelengths. These frequency downshifted photons slip back due to dispersion with a velocity  $v_{\text{etch}} = c\omega_p^2/\omega_0^2$  into the wake where the transverse density depression is sufficient for guiding them. Here,  $v_{\text{etch}}$  is the difference between the linear and nonlinear group velocity of the laser pulse [11]. This considerably reduces the loss from diffractive erosion and leads to an enhanced  $a_0$  from the downshifted photons at the head of the laser pulse [2]. This, in turn, helps maintain a strong plasma wake over many  $Z_R$ . Ultimately, energy transfer from the laser to the wake limits the length over which such a pulse can be self-guided by the plasma [2,11]. To the first order, this nonlinear pump depletion length  $L_{\text{pd}}$  is given as [10],

$$L_{\text{pd}} = \frac{c}{v_{\text{etch}}}(c\tau) \approx \frac{\omega_o^2}{\omega_p^2}(c\tau) \propto \frac{1}{n_e}. \quad (1)$$

For  $2 < a_0 < 20$ , this scaling is independent of  $a_0$ , and therefore independent of power as long as  $P/P_c > 1$ . Beyond the pump depletion limit, the pulse is so severely etched that it is no longer intense enough to excite a wake and therefore no longer guided.

Experiments reported here were conducted using a Ti:sapphire laser system capable of providing up to 12 TW,  $50 \pm 5$  fs FWHM laser pulses with a central wavelength of  $0.815 \mu\text{m}$ . The targets used were four different diameter (2, 3, 5, and 8.5 mm) supersonic helium gas jets [18]. For each shot, the laser energy and pulse length were monitored. Plasma was produced via tunnel ionization by the laser field [19]. Plasma interferometry carried out with a 65 fs transverse probe pulse revealed no ionization due to any residual prepulse.

The laser pulse was focused using a  $f/5$  off-axis parabola to a  $w_o$  of  $5.5 \mu\text{m}$  giving a  $Z_R$  of  $115 \mu\text{m}$ . Measurements show that about  $\sim 60\%$  of the laser energy is contained within this  $w_o$ . After accounting for this energy difference and using the measured pulse lengths, the typical range of focused intensities correspond to  $1.3 < a_0 < 3.5$  for these experiments.

The experimental setup is illustrated in the inset to Fig. 1. A detailed schematic including diagnostics can be found in Ref. [20]. Most of the results discussed here were obtained using the 5 mm gas jet; the other gas jets gave qualitatively similar results. The plasma density profile was measured by interferometry and is also shown in the Fig. 1 inset. Within the  $\pm 1 \times 10^{18} \text{ cm}^{-3}$  errors, an on-axis density profile was found which is constant over  $4.9 \pm 0.2$  mm and having entrance and exit ramp lengths of  $\sim 150 \mu\text{m}$ . By varying the gas-jet nozzle's backing pressure, plasma densities ranging from  $4 \times 10^{18}$  to  $1 \times 10^{19} \text{ cm}^{-3}$  could be produced. For this density range,  $w_m$  varies from 8 to  $4 \mu\text{m}$ . The parameter  $P/P_c$  was varied by

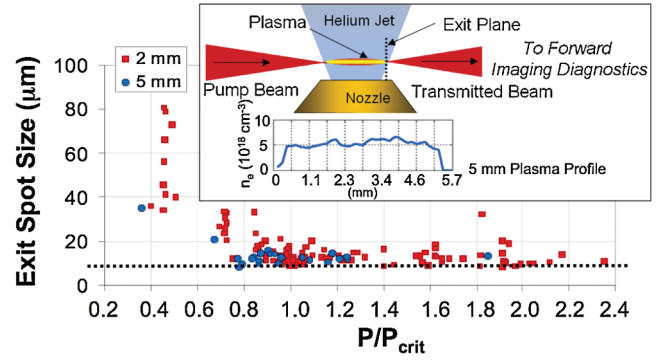


FIG. 1 (color). The  $1/e^2$  radius laser spot size measured at the exit of the plasma vs  $P/P_c$  for 2 and 5 mm long gas-jet targets. The dotted line is the resolution limit. The experimental arrangement is illustrated in the inset. Also shown is a typical 5 mm jet plasma density profile.

varying the combination of  $n_e$  and  $P$ . For the range of plasma densities, the laser pulse length of 50 fs corresponds to  $0.8\lambda_w < c\tau < 1.2\lambda_w$ , where  $\lambda_w \approx \frac{4c}{w_p} \sqrt{a_0}$  is the nonlinear wavelength of the first wake period [2]. The laser photons transmitted by the plasma were collected and sent to two independent, imaging diagnostics. One of these provided a relayed image of either the entrance or the exit of the gas jet in use and was measured with a 12 bit CCD camera. The observed variation of the mean spot size at the plasma exit versus  $P/P_c$  for plasmas produced using 2 and 5 mm long gas-jet nozzles is shown in Fig. 1. In both cases, the spot size shows a decrease from its vacuum spot size for  $P/P_c > 0.4$ . The minimum measured spot size of  $10 \mu\text{m}$ , reached at  $P/P_c \approx 1$ , is limited by the optical imaging system.

The laser spot images in vacuum at the entrance and exit of the 5 mm nozzle are shown in Figs. 2(a) and 2(b), respectively. Note that the  $\approx 160 \mu\text{m}$  spot in Fig. 2(b) is much larger than those plotted in Fig. 1. Figures 2(c)–2(f) show images of the laser spot at the exit of the 5 mm long plasma (gas jet on) as  $n_e$  is increased. At  $n_e = 4 \times 10^{18} \text{ cm}^{-3}$  and  $P/P_c \approx 0.6$ , a hint of a well-guided spot (black lineout) first appears, although it is surrounded by a halo of diffracted light (white lineout) as seen in Fig. 2(c). As  $n_e$  is increased to  $6 \times 10^{18} \text{ cm}^{-3}$  and to  $P/P_c$  to 1, the guided spot becomes more pronounced compared with the halo surrounding it, as shown in Fig. 2(d). Best guiding is observed for a density of  $7 \times 10^{18} \text{ cm}^{-3}$  and  $P/P_c \approx 1$  as shown in Fig. 2(e). Here  $w_o \approx w_m$ . Relative to the peak intensity, there is very little intensity in the surrounding halo since the black and white lineouts are almost identical. As  $n_e$  is further increased to  $8 \times 10^{18} \text{ cm}^{-3}$ , the fraction of the transmitted energy that is contained in the guided spot clearly decreases (i.e., the halo reappears) as seen in Fig. 2(f). This is thought to be due to a combination of continuous diffraction of the head of the pulse (beam head erosion) and energy depletion to the wake (pump depletion). We have determined that the

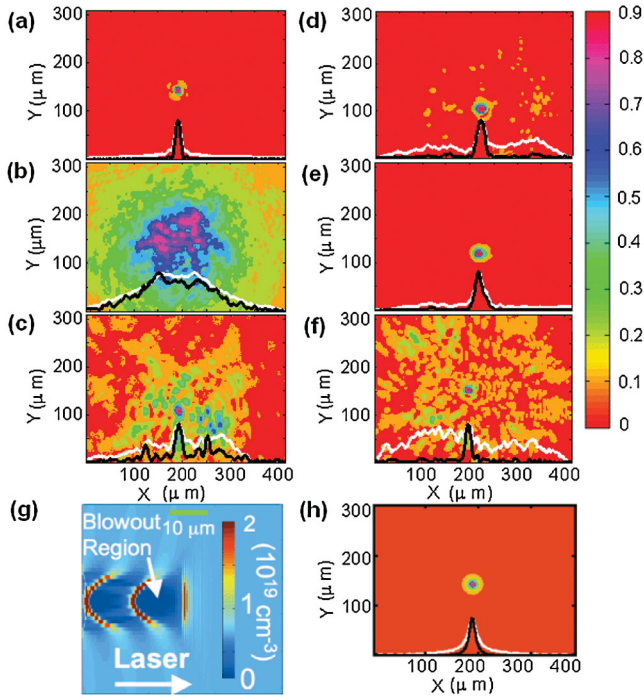


FIG. 2 (color). Images of the laser spot at vacuum best focus (a) and after 5 mm in vacuum (b). Parts (c)–(f) are images of the spot at the exit of the 5 mm plasma with densities of 4, 6, 7, and  $8 \times 10^{18} \text{ cm}^{-3}$ , respectively. White curves are lineouts in the  $x$  direction after summing in the  $y$  direction, whereas the black curves are a lineout through the center of the guided spot from which the spot size at the exit is obtained. Parts (g), (h) show results from 3D PIC simulation for the case shown in (e). Density at 3.3 mm (g) and exit laser spot (h).

guided spot in Fig. 2(e) contained  $\sim 70\%$  of the total transmitted energy in the laser pulse. The efficacy of self-guiding for this initial  $5.5 \mu\text{m}$  spot falls off for both higher and lower densities from a peak where the density, power, and spot size are matched.

Results of three-dimensional simulations of the experimental matched conditions using the particle-in-cell (PIC) code OSIRIS are shown in Figs. 2(f) and 2(h). An example of electron blowout in the first plasma period as seen throughout this simulation is shown in Fig. 2(g). Here the pulse has propagated a distance 3.3 mm ( $28 Z_R$ ). Figure 2(h) shows a forward image of the simulation laser pulse at the end of 5 mm which is directly analogous to Figs. 2(c)–2(f). As in the experiment [Fig. 2(e)], the simulation spot is well defined with little halo.

The second forward imaging system is nearly identical to that used for the data in Fig. 2 except that the image is formed onto the slit of an imaging spectrograph with a wavelength resolution of 7 nm and spatial resolution of  $\sim 15 \mu\text{m}$ . The resulting imaged spectra, corrected for the  $\lambda$ -dependent transmission of the imaging optics, are shown in Figs. 3(a)–3(c). The corresponding Figs. 3(d)–3(f) have been normalized to 1 within each spectral bin. This procedure brings out the spectral content of the halo which,

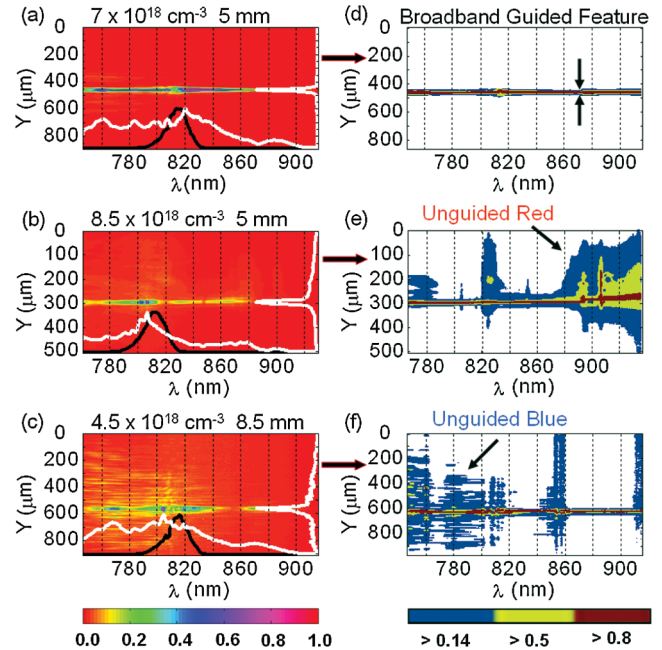


FIG. 3 (color). Here (a)–(c) are the spectra of the pulse imaged at the exit of each gas jet. Corresponding parts (d)–(f) have been normalized along each spectral bin to accentuate which wavelengths are guided. The white curve along the side ( $Y$ ) is the spectrally integrated spatial distribution. The white curve along  $\lambda$  is the spatially integrated spectrum. The black curve is the initial pulse spectrum.

although it is not very intense, can contain a significant amount of the total energy in the pulse spread over a much wider area.

In Figs. 3(a)–3(c), the spectral content of the resolution limited guided spot is recognized as the narrow feature stretching across the entire range of the spectrometer. The white curve along the side reveals the spatial size and total energy contrast of this guided feature for each of the three cases. Since  $c\tau \sim \lambda_p$  for this range of  $n_e$ , spectral modulation must come from the interaction of the laser pulse with the first plasma period. Compared with the initial normalized spectrum of the laser (black curve), the white curve along  $\lambda$  shows photon acceleration at the back of the pulse which leads to a blueshift and pump depletion at the front of the pulse which redshifts the photons [21]. This spatially narrow but spectrally broad feature is evidence for the existence of the laser pulse residing within a large amplitude wake throughout the full length of the plasma and thus of self-guiding.

In Figs. 3(a) and 3(d), the spectrum of the light exiting a 5 mm long,  $7 \times 10^{18} \text{ cm}^{-3}$  plasma is shown. This is where Fig. 2(d) showed the highest contrast between the guided spot and the surrounding halo. These spectral images show that the spectral range is confined only to the narrow, guided region which indicates optimal self-guiding. As the density is increased to  $8.5 \times 10^{18} \text{ cm}^{-3}$ , the frequency content of the guided portion of the laser pulse, Fig. 3(b), is

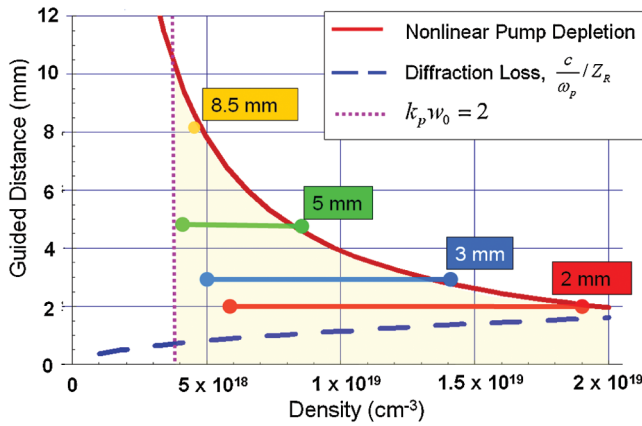


FIG. 4 (color). Summary of densities where self-guiding was observed by forward exit imaging and associated forward spectrum in each of the four gas jets. The solid red curve is the plot of Eq. (1) for a 55 fs laser pulse.

qualitatively similar to that in Fig. 3(a). However, the normalized spectrum of Fig. 3(e) shows that some of the redshifted photons (which have lost energy to the wake) are spread over a wider area because of diffraction. This enhanced diffraction near the front of the pulse suggests that the laser pulse is near  $L_{pd}$  for this  $n_e$  as expected from Eq. (1). Because of the now reduced contrast between the guided and unguided portions of the pulse, the weak, ionization blueshifted photons [22] at the very front of the pulse are now visible.

To achieve a degree of self-guiding over 8.5 mm, a lower  $n_e$  of  $4.5 \times 10^{18} \text{ cm}^{-3}$  was used to avoid pump depletion as described in Eq. (1). Additionally, the laser power was increased to maintain  $P/P_c \geq 1$ . For this  $n_e$ ,  $w_o < w_m$ , and thus most of the laser pulse could not be self-guided. As seen in Figs. 3(c) and 3(f), the spectrum of the transmitted light once again shows the usual broadband and spatially narrow, but now, weakly guided feature. In addition, however, the broad unguided feature seen in Fig. 3(e) is now all ionization blueshifted.

In Fig. 4, the range of densities over which self-guiding was observed for gas jets of different lengths is plotted. The yellow shaded area defines the area where guiding is expected to occur. Here the highest density is bounded by  $L_{pd}$  (the solid red curve), while the lowest density is bounded by the required density channel depth (dotted pink line). For the case of complete cavitation, the required depth  $\delta n/n_e$  is limited by  $n_e$ , such that  $k_p w_o \geq 2$ ; i.e.,  $n_e > 4 \times 10^{18} \text{ cm}^{-3}$  for our  $w_o$ . The maximum propagation length for a laser pulse which erodes due to diffraction by a distance of  $c/\omega_p$  per initial  $Z_R$  is also plotted (dashed blue curve). All observed self-guided lengths exceed this sup-

posed limitation. Instead, the maximum  $n_e$  points where self-guiding was measured for all the plasma lengths are consistent with the limitations imposed by the Eq. (1) scaling. At the highest densities,  $c\tau > \lambda_w$ , and pulse evolution must happen before the experiment is in the blowout, LWFA regime. However, since at these highest densities, where  $P/P_c \gg 1$ , this occurs rapidly. At the lowest densities, while  $c\tau < \lambda_w$ , the self-guiding process is limited by a drop in the maximum value of  $\delta n/n_e$  as well as a reduction of  $P/P_c$ .

In conclusion, experimental results demonstrate self-guiding of intense but ultrashort laser pulses over tens of  $Z_R$  in a plasma. The observed self-guiding is most effective when  $w_o$  is matched to the blowout radius  $R_b$ . The beam head erosion rate due to diffraction is considerably less than the simple estimate of  $c/\omega_p$  per  $Z_R$ . The ultimate limit of self-guided propagation distance in the blowout regime is the pump depletion of the laser pulse.

This work was supported by The Department of Energy Grant No. DEFG02-92ER40727.

- 
- [1] T. Tajima and J. Dawson, Phys. Rev. Lett. **43**, 267 (1979).
  - [2] W. Lu *et al.*, Phys. Plasmas **13**, 056709 (2006).
  - [3] C. G. Durfee and H. M. Milchberg, Phys. Rev. Lett. **71**, 2409 (1993).
  - [4] A. Butler *et al.*, Phys. Rev. Lett. **89**, 185003 (2002).
  - [5] C. G. R. Geddes *et al.*, Phys. Rev. Lett. **95**, 145002 (2005).
  - [6] Proceedings of the Advanced Accelerator Concepts, 2008 (AIP, to be published).
  - [7] A. G. R. Thomas *et al.*, Phys. Rev. Lett. **98**, 095004 (2007).
  - [8] G. M. A. Chiron *et al.*, Phys. Plasmas **3**, 1373 (1996).
  - [9] T.-W. Yau *et al.*, Phys. Plasmas **9**, 391 (2002).
  - [10] W. Lu *et al.*, Phys. Rev. ST Accel. Beams **10**, 061301 (2007).
  - [11] C. D. Decker *et al.*, Phys. Plasmas **3**, 2047 (1996).
  - [12] A. Pukhov and J. Meyer ter veht, Appl. Phys. B **74**, 355 (2002).
  - [13] J. Faure *et al.*, Phys. Plasmas **9**, 756 (2002).
  - [14] E. Esarey *et al.*, IEEE Trans. Plasma Sci. **24**, 252 (1996).
  - [15] G.-Z. Sun *et al.*, Phys. Fluids **30**, 526 (1987).
  - [16] P. Sprangle *et al.*, Phys. Rev. Lett. **64**, 2011 (1990).
  - [17] W. Lu *et al.*, Phys. Rev. Lett. **96**, 165002 (2006).
  - [18] S. Semushin and V. Malka, Rev. Sci. Instrum. **72**, 2961 (2001).
  - [19] L. V. Keldysh, Sov. Phys. J. Exp. Theor. Phys. **20**, 1307 (1965).
  - [20] J. E. Ralph *et al.*, in *IEEE Particle Accelerator Conference Proceedings* (IEEE, New York, 2007), pp. 2296–2298.
  - [21] D. F. Gordon *et al.*, Phys. Rev. Lett. **90**, 215001 (2003).
  - [22] Wm. M. Wood *et al.*, Opt. Lett. **13**, 984 (1988).